

Molecular Structures of Supported Niobium Oxide Catalysts under in Situ Conditions

Jih-Mirn Jehng and Israel E. Wachs*

Zettlemoyer Center for Surface Studies, Department of Chemical Engineering, Lehigh University, Bethlehem, Pennsylvania 18015 (Received: October 12, 1990)

Supported niobium oxide catalysts were investigated by in situ Raman spectroscopy as a function of Nb₂O₅ loading and oxide support (MgO, Al₂O₃, TiO₂, ZrO₂, and SiO₂) in order to determine the molecular structures of the dehydrated surface niobium oxide species. On the SiO₂ support, only one dehydrated surface niobium oxide species corresponding to the highly distorted NbO₆ octahedral structure at ~980 cm⁻¹ is present. The highly distorted NbO₆ octahedra responsible for Raman bands at ~985 and ~935 cm⁻¹ are also observed on the TiO₂ and ZrO₂ supports at high surface coverages; however, the dehydrated surface niobium oxide phases possessing Raman bands in the 600–700-cm⁻¹ region cannot be directly observed for Nb₂O₅/TiO₂ and Nb₂O₅/ZrO₂ because of the strong vibrations of the oxide supports in this region. Below half a monolayer coverage on the Al₂O₃ support, two kinds of dehydrated surface niobium oxide species possessing highly and moderately distorted NbO₆ octahedra with Nb=O Raman bands at ~980 and ~883 cm⁻¹, respectively, are present. Upon approaching monolayer coverage on the Al₂O₃ support, additional Raman bands at ~935 and ~647 cm⁻¹ characteristic of highly and slightly distorted NbO₆ octahedra are present and are suggestive of a layered niobium oxide structure. Multiple niobium oxide species are present in the Nb₂O₅/MgO system and are due to the strong acid–base interactions between Nb₂O₅ and Mg²⁺ as well as Ca²⁺ impurity cations present on the surface. The various dehydrated surface niobium oxide species present in the supported niobium oxide catalysts appear to be related to the oxide support surface hydroxyl chemistry.

Introduction

Recent studies of supported metal oxide catalysts have revealed that the supported metal oxide phase forms a two-dimensional metal oxide overlayer on oxide supports such as Al₂O₃, TiO₂, and SiO₂.^{1–7} These surface metal oxide phases possess different chemical states, which may simultaneously be present on the support surface, than their bulk metal oxide crystallites. The different chemical states of the surface metal oxide phases can be discriminated with Raman spectroscopy because each state possesses a unique vibrational spectrum corresponding to its structure.^{8,9} Additional fundamental information about the supported metal oxide catalysts is provided by in situ Raman spectroscopy since this technique provides structural information about the surface metal oxide phases under a controlled environment (temperature and gas-phase composition).^{8–11}

The molecular structures of supported vanadium oxide on Al₂O₃, TiO₂, and SiO₂ supports have been extensively characterized under in situ conditions, where the surface metal oxide phases are dehydrated, with Raman spectroscopy,^{12–15} infrared spectroscopy,¹⁶ and ⁵¹V NMR spectroscopy,¹⁷ as well as XANES.¹⁸ Upon dehydration, the surface vanadium oxide Raman bands above 800 cm⁻¹, which are characteristic of the V=O symmetric stretch, split into a sharp Raman band in the 1026–1038-cm⁻¹

region and a broad Raman band at ~900 cm⁻¹. The relative intensity of these two Raman bands varies with surface vanadium oxide coverage on the oxide supports.^{10,12,13} However, the V₂O₅/SiO₂ system only possesses a single Raman band at ~1038 cm⁻¹.¹² Raman and ⁵¹V NMR studies suggest that the dehydrated surface vanadium oxide phases are present as a monoxo tetrahedral vanadate species (Raman band in the 1026–1038-cm⁻¹ region) and a polymeric tetrahedral metavanadate species (Raman band at ~900 cm⁻¹).¹⁹ In situ IR studies also suggest that the dehydrated surface vanadium oxide species are present as an isolated vanadate species (IR band in the 1030–1050 cm⁻¹) and a polyvanadate species (expected IR band in the 600–800 cm⁻¹).¹⁶ In addition, in situ Raman studies on Al₂O₃, TiO₂, and SiO₂ supported molybdenum oxide and tungsten oxide catalysts also exhibit Raman shifts of the surface molybdenum oxide (from ~950 to 985–1012 cm⁻¹)^{10,20–22} and the surface tungsten oxide (from ~960 to 1010–1027 cm⁻¹).^{8,10,20,23–25} phases due to dehydration of the surface metal oxide phases. In situ XANES/EXAFS studies on SiO₂ and Al₂O₃ supported vanadium oxide catalysts reveal that the hydrated vanadium oxide species on SiO₂ possess a polymeric octahedral structure which transforms into a monoxo tetrahedral vanadate structure upon dehydration, and both hydrated and dehydrated vanadium oxide species on Al₂O₃ possess an isolated tetrahedral structure at low surface coverages.¹⁸

Raman and XPS studies on the supported niobium oxide catalysts under ambient conditions reveal that the surface niobium oxide phase forms a two-dimensional overlayer on oxide supports (MgO, Al₂O₃, TiO₂, ZrO₂, and SiO₂), and the monolayer coverage of supported niobium oxide catalysts is reached at ~19 wt % Nb₂O₅/Al₂O₃, ~7 wt % Nb₂O₅/TiO₂, ~5 wt % Nb₂O₅/ZrO₂, and ~2 wt % Nb₂O₅/SiO₂, but not for the Nb₂O₅/MgO system due to the incorporation of Nb⁵⁺ into the MgO support.⁷ The molecular structures of the surface niobium oxide phases are controlled by the surface pH of the system. Basic hydrated surfaces result in the formation of highly distorted NbO₆ groups and acidic hydrated surfaces result in the formation of slightly

(1) Wachs, I. E.; Jehng, J. M.; Hardcastle, F. D. *Solid State Ionics* 1989, 32/33, 904.(2) Murrell, L. L.; Grenoble, D. C.; Kim, C. J.; Dispenziere, N. C. *J. Catal.* 1987, 107, 463.(3) Nishimura, M.; Asakura, K.; Iwasawa, Y. *J. Chem. Soc., Chem. Commun.* 1986, 1660.(4) Nishimura, M.; Asakura, K.; Iwasawa, Y. *Proc. 9th Int. Congr. Catal.* 1988, 4, 1842.(5) Shirai, M.; Ichikuni, N.; Asakura, A.; Iwasawa, Y. *Catal. Today* 1990, 8(1), 57.(6) Weissman, J. G.; Ko, E. I.; Wynblatt, P. *J. Catal.* 1987, 108, 383.(7) Jehng, J. M.; Wachs, I. E. *J. Mol. Catal.* 1991, 67, 369.(8) Wachs, I. E.; Hardcastle, F. D.; Chan, S. S. *Spectroscopy* 1986, 1, 30.(9) Stencel, J. M. *Raman Spectroscopy for Catalysis*; Van Nostrand Reinhold: New York, 1990.(10) Chan, S. S.; Wachs, I. E.; Murrell, L. L.; Wang, L.; Hall, W. K. *J. Phys. Chem.* 1984, 88, 5831.

(11) Wang, L. Ph.D. Dissertation, University of Wisconsin—Milwaukee, 1982.

(12) Deo, G.; Eckert, H.; Wachs, I. E. *Prepn.—Am. Chem. Soc., Div. Pet. Chem.* 1990, 35(1), 16.

(13) Deo, G.; Vuorman, M.; Wachs, I. E., to be published.

(14) Went, G. T.; Oyama, S. T.; Bell, A. T. *J. Phys. Chem.* 1990, 94, 4240.(15) Oyama, S. T.; Went, G. T.; Lewis, K. B.; Bell, A. T.; Somarjai, G. *J. Phys. Chem.* 1989, 93, 6786.(16) Cristinai, C.; Forzatti, P.; Busca, G. *J. Catal.* 1989, 116, 586.(17) Eckert, H.; Wachs, I. E. *J. Phys. Chem.* 1989, 93, 6796.(18) Yoshida, S.; Tanaka, T.; Nishimura, Y.; Mizutani, H.; Funabiki, T. *Proc. 9th Int. Congr. Catal.* 1988, 3, 1473.(19) Wachs, I. E. *J. Catal.* 1990, 124, 570.

(20) Machej, T.; Haber, J.; Turek, A. W.; Wachs, I. E., to be published.

(21) Stencel, J. M.; Makovsky, L. E.; Sarkus, T. A.; de Vries, J.; Thomas, R.; Moulijn, J. *J. Catal.* 1984, 90, 314.(22) Stencel, J. M.; Diehl, J. R.; D'Este, J. R.; Makovsky, L. E.; Rodrigo, L.; Marcinkowska, K.; Adnot, A.; Roberge, P. C.; Kaliaguine, S. *J. Phys. Chem.* 1986, 90, 4739.(23) Chan, S. S.; Wachs, I. E.; Murrell, L. L.; Dispenziere, N. C. *J. Catal.* 1985, 92, 1.(24) Chan, S. S.; Wachs, I. E.; Murrell, L. L. *J. Catal.* 1984, 90, 150.(25) Stencel, J. M.; Makovsky, L. E.; Diehl, J. R.; Sarkus, T. A. *J. Raman Spectrosc.* 1984, 15, 282.

distorted NbO_6 , NbO_7 , and NbO_3 groups (with the exception of the $\text{Nb}_2\text{O}_5/\text{SiO}_2$ system which forms bulk Nb_2O_5). The molecular structures of the dehydrated surface niobium oxide phases, however, are still not understood and only preliminary in situ XANES studies for silica-supported niobium oxide catalysts have been reported by Yoshida et al.²⁶ In the present study, the MgO , Al_2O_3 , TiO_2 , ZrO_2 , and SiO_2 supported niobium oxide catalysts will be investigated under in situ conditions with Raman spectroscopy in order to determine the molecular structures of the dehydrated surface niobium oxide phases as a function of Nb_2O_5 loading and the specific oxide support.

Experimental Section

a. Materials and Preparations. Niobium oxalate was supplied by Niobium Products Co. (Pittsburgh, PA) with the following chemical analysis: 20.5% Nb_2O_5 , 790 ppm Fe, 680 ppm Si, and 0.1% insolubles. Niobium ethoxide (99.999% purity) was purchased from Johnson Matthey (Ward Hill, MA). The oxide supports employed in the present investigation are MgO (Fluka, $\sim 80 \text{ m}^2/\text{g}$ after calcination at 700°C for 2 h), Al_2O_3 (Harshaw, $\sim 180 \text{ m}^2/\text{g}$ after calcination at 500°C for 16 h), TiO_2 (Degussa, $\sim 50 \text{ m}^2/\text{g}$ after calcination at 450°C for 2 h), ZrO_2 (Degussa, $\sim 39 \text{ m}^2/\text{g}$ after calcination at 450°C for 2 h), and SiO_2 (Cab-O-Sil, $\sim 275 \text{ m}^2/\text{g}$ after calcination at 500°C for 16 h).

The TiO_2 , ZrO_2 , Al_2O_3 , and SiO_2 supported niobium oxide catalysts were prepared by the incipient-wetness impregnation method using niobium oxalate/oxalic acid aqueous solutions (aqueous preparation).²⁷ The water-sensitive MgO support required the use of nonaqueous niobium ethoxide/propanol solutions under a nitrogen environment for the preparation of the $\text{Nb}_2\text{O}_5/\text{MgO}$ catalysts.

For the aqueous preparation method the samples were initially dried at room temperature for 16 h, further dried at $110\text{--}120^\circ\text{C}$ for 16 h, and subsequently calcined at 450°C ($\text{Nb}_2\text{O}_5/\text{TiO}_2$ and $\text{Nb}_2\text{O}_5/\text{ZrO}_2$, 2 h) or at 500°C ($\text{Nb}_2\text{O}_5/\text{Al}_2\text{O}_3$ and $\text{Nb}_2\text{O}_5/\text{SiO}_2$, 16 h) under flowing dry air. For the nonaqueous preparation method, the samples were initially dried at room temperature for 16 h, further dried at $110\text{--}120^\circ\text{C}$ for 16 h under flowing N_2 , and subsequently calcined at 500°C for 1 h under flowing N_2 then for 1 h under flowing dry air.

b. In Situ Raman Spectroscopy. The in situ Raman spectrometer consists of a quartz cell and sample holder, a triple-grating spectrometer (SPEX, Model 1877), a photodiode array detector (EG&G, Princeton Applied Research, Model 1420), and an argon ion laser (Spectra-Physics, Model 171). The sample holder is made from a quartz glass, and a 100–200-mg sample disk is held by a stationary slot in the sample holder. The sample is heated by a cylindrical heating coil surrounding the quartz cell, and the temperature is measured with an internal thermocouple. The quartz cell is capable of operating up to 600°C , and dry oxygen gas (Linde Specialty Grade, 99.99% purity) is introduced into the cell at a rate of $50\text{--}500 \text{ cm}^3/\text{min}$ with a delivery pressure of 150–200 torr.

The Raman spectra are collected for the hydrated sample at room temperature, after heating the sample to 500°C in flowing oxygen for 30 min, and again after cooling down to 50°C to avoid the thermal broadening of Raman bands at high temperature. The laser beam 514.5-nm line of the Ar^+ laser with 10–100 mW of power is focused on the sample disk in a right-angle scattering geometry. An ellipsoid mirror collects and reflects the scattering light into the spectrometer's filter stage to reject the elastic scattering. The resulting filtered light, consisting primarily of the Raman component of the scattered light, is collected with an EG&G intensified photodiode array detector which is coupled to the spectrometer and is thermoelectrically cooled to -35°C . The photodiode array detector is scanned with an EG&G OMA III optical multichannel analyzer (Model 1463). The Raman spec-

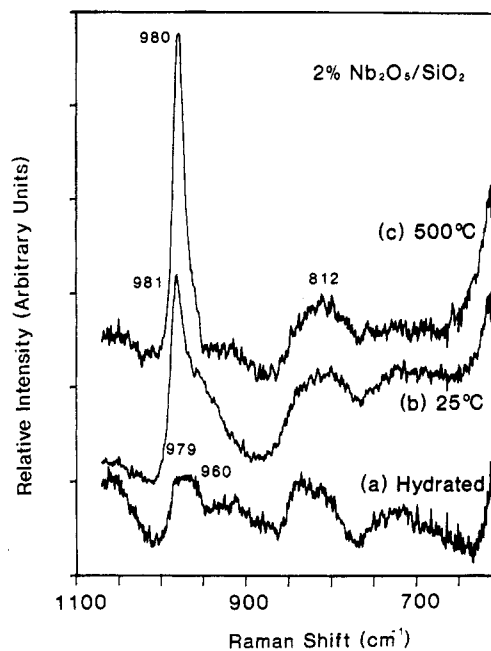


Figure 1. In situ Raman spectra of 2 wt % $\text{Nb}_2\text{O}_5/\text{SiO}_2$: (a) hydrated state; (b) collected at 25°C (fresh from the oven at 500°C); (c) heated at 500°C under flowing oxygen.

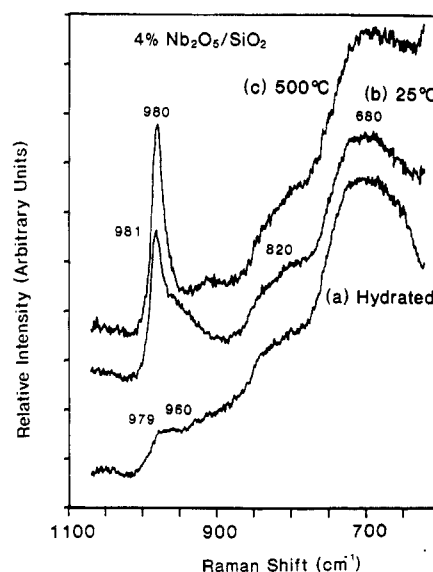


Figure 2. In situ Raman spectra of 4 wt % $\text{Nb}_2\text{O}_5/\text{SiO}_2$: (a) hydrated state; (b) collected at 25°C (fresh from the oven at 500°C); (c) heated at 500°C under flowing oxygen.

trum is recorded only in the high-wavenumber region ($600\text{--}1100 \text{ cm}^{-1}$) in the present experiments. The overall resolution of the spectra was determined to be better than 1 cm^{-1} .

Results

$\text{Nb}_2\text{O}_5/\text{SiO}_2$. The in situ Raman spectra of the silica-supported niobium oxide were collected at 25°C (fresh from the oven) and 500°C in the closed cell because intense fluorescence occurred after the samples were cooled down to 50°C in the cell. The hydrated spectra were obtained after exposing the sample to ambient conditions for overnight. The SiO_2 support possesses Raman bands at ~ 979 and $\sim 812 \text{ cm}^{-1}$ which are characteristic of the Si–OH stretch and Si–O–Si linkages.²⁸ The hydrated surface niobium oxide phase possessing a weak Raman band at $\sim 960 \text{ cm}^{-1}$ shifts to $\sim 980 \text{ cm}^{-1}$ upon dehydration as shown in Figures 1 and 2. Thus, the Raman spectrum collected at 25°C

(26) Yoshida, S.; Nishimura, Y.; Tanaka, T.; Kanai, H.; Funabiki, T. *Catal. Today* **1990**, *3*(1), 67.

(27) Jehng, J. M.; Wachs, I. E. *Prepn.—Am. Chem. Soc., Div. Pet. Chem.* **1989**, *34*(3), 546.

(28) Tallent, D. R.; Bunker, B. C.; Brinker, C. J.; Balfe, C. A. In *Better Ceramics Through Chemistry II*; Brinker, C. J., Clark, D. E., Ulrich, D. R., Eds.; Materials Research Society: Pittsburgh, 1986; pp 261.

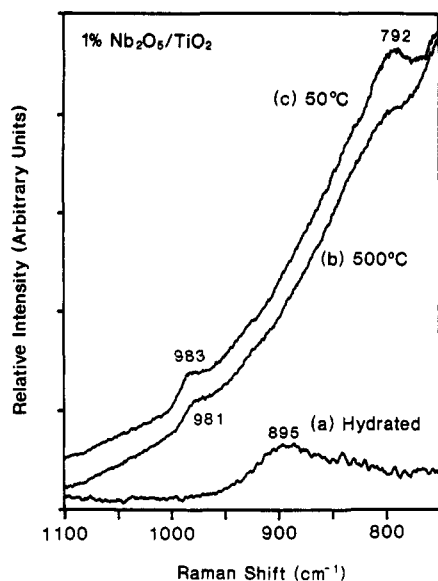


Figure 3. In situ Raman spectra of 1 wt % $\text{Nb}_2\text{O}_5/\text{TiO}_2$: (a) hydrated state (subtracted TiO_2 background in the $750\text{--}1100\text{-cm}^{-1}$ region); (b) heated at $500\text{ }^\circ\text{C}$ under flowing oxygen; (c) cooled to $50\text{ }^\circ\text{C}$ under flowing oxygen.

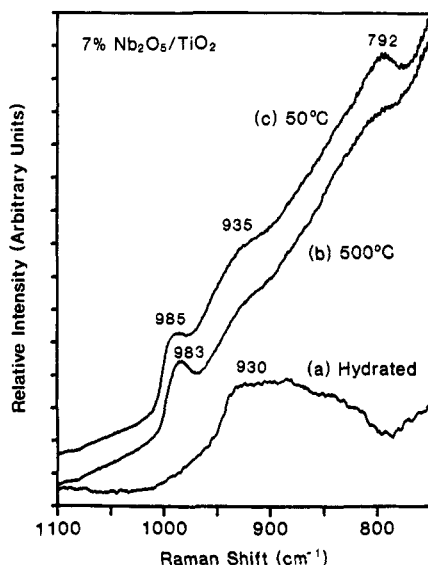


Figure 4. In situ Raman spectra of 7 wt % $\text{Nb}_2\text{O}_5/\text{TiO}_2$: (a) hydrated state (subtracted TiO_2 background in the $750\text{--}1100\text{-cm}^{-1}$ region); (b) heated at $500\text{ }^\circ\text{C}$ under flowing oxygen; (c) cooled to $50\text{ }^\circ\text{C}$ under flowing oxygen.

(fresh from the oven) possessing both a sharp Raman band at $\sim 980\text{ cm}^{-1}$ and a broad Raman band at $\sim 960\text{ cm}^{-1}$ indicates that the surface niobium oxide phase is partially dehydrated. For the 4 wt % $\text{Nb}_2\text{O}_5/\text{SiO}_2$ sample, an additional Raman band is present at $\sim 680\text{ cm}^{-1}$ and does not shift under the in situ conditions.

$\text{Nb}_2\text{O}_5/\text{TiO}_2$. The dehydration of the 1 wt % $\text{Nb}_2\text{O}_5/\text{TiO}_2$ sample reveals that the hydrated supported niobium oxide phase possessing a very weak and broad Raman band at $\sim 895\text{ cm}^{-1}$ shifts to $\sim 983\text{ cm}^{-1}$ as shown in Figure 3. The disappearance of the weak Raman band at $\sim 792\text{ cm}^{-1}$ at $500\text{ }^\circ\text{C}$, the first overtone of the Raman band at $\sim 394\text{ cm}^{-1}$ of TiO_2 , is due to the thermal broadening of the crystalline TiO_2 phase. Upon increasing the Nb_2O_5 loading to 7 wt %, an additional weak and broad Raman band appears at $\sim 935\text{ cm}^{-1}$ upon dehydrating the supported niobium oxide phase as shown in Figure 4.

$\text{Nb}_2\text{O}_5/\text{ZrO}_2$. The in situ Raman spectra of the zirconia-supported niobium oxide catalysts are presented in Figures 5 and 6 with different Nb_2O_5 loadings. The ZrO_2 support possesses a weak Raman band at $\sim 756\text{ cm}^{-1}$ which arises from the first overtone of its strong Raman band at $\sim 380\text{ cm}^{-1}$. The thermal effect on

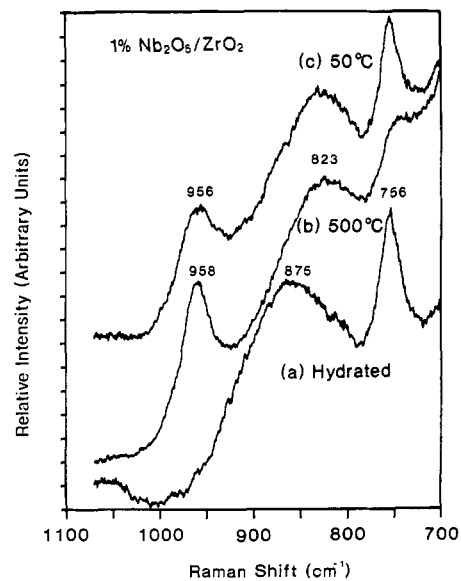


Figure 5. In situ Raman spectra of 1 wt % $\text{Nb}_2\text{O}_5/\text{ZrO}_2$: (a) hydrated state; (b) heated at $500\text{ }^\circ\text{C}$ under flowing oxygen; (c) cooled to $50\text{ }^\circ\text{C}$ under flowing oxygen.

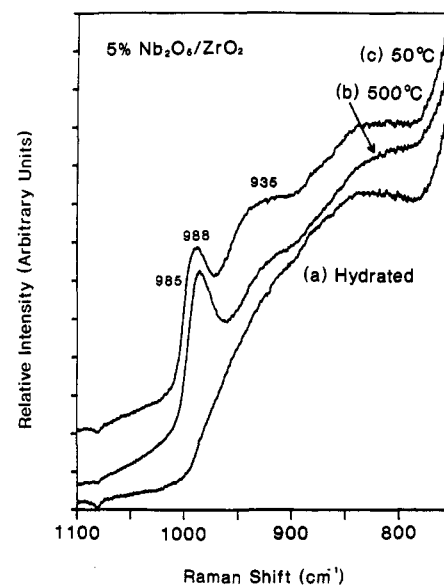


Figure 6. In situ Raman spectra of 5 wt % $\text{Nb}_2\text{O}_5/\text{ZrO}_2$: (a) hydrated state; (b) heated at $500\text{ }^\circ\text{C}$ under flowing oxygen; (c) cooled to $50\text{ }^\circ\text{C}$ under flowing oxygen.

the Raman scattering cross section of this band is similar to TiO_2 . For the 1 wt % $\text{Nb}_2\text{O}_5/\text{ZrO}_2$ sample, the hydrated supported niobium oxide phase possesses a weak and broad Raman band at $\sim 875\text{ cm}^{-1}$ which shifts to ~ 958 and $\sim 823\text{ cm}^{-1}$ upon dehydration (see Figure 8). For the 5 wt % $\text{Nb}_2\text{O}_5/\text{ZrO}_2$ sample, the dehydrated surface niobium oxide Raman bands appear at ~ 988 , ~ 935 , and $\sim 823\text{ cm}^{-1}$.

$\text{Nb}_2\text{O}_5/\text{Al}_2\text{O}_3$. The in situ Raman spectra of the alumina-supported niobium oxide containing 5 and 19 wt % Nb_2O_5 are shown in Figures 7 and 8, respectively. For the 5 wt % Nb_2O_5 loading, a broad and weak Raman band due to the surface niobium oxide phase (since the Al_2O_3 support is not Raman active) appears at $\sim 905\text{ cm}^{-1}$ under ambient conditions, and shifts to ~ 980 and $\sim 883\text{ cm}^{-1}$ upon surface dehydration. For the 19 wt % Nb_2O_5 loading, the hydrated sample exhibits Raman bands at ~ 890 and $\sim 645\text{ cm}^{-1}$ due to the hydrated surface niobium oxide phases on the alumina support. Upon dehydration, the Raman band at $\sim 890\text{ cm}^{-1}$ shifts to ~ 988 , ~ 935 , and $\sim 883\text{ cm}^{-1}$ and the Raman band at $\sim 645\text{ cm}^{-1}$, however, remains at the same position.

The Raman spectra of the dehydrated surface niobium oxide phases on alumina are also shown in Figure 9 as a function of Nb_2O_5 loading. For the loadings less than 5 wt % Nb_2O_5 , only

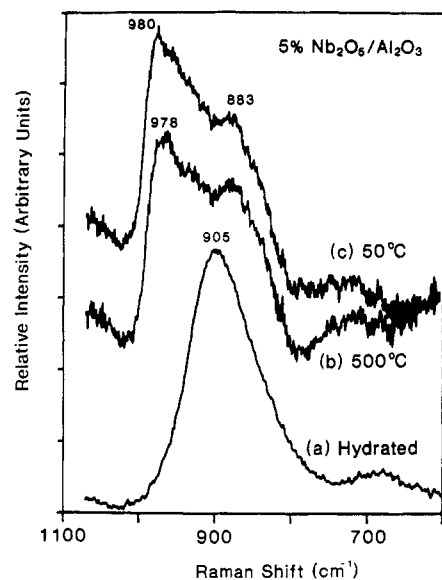


Figure 7. In situ Raman spectra of 5 wt % $\text{Nb}_2\text{O}_5/\text{Al}_2\text{O}_3$: (a) hydrated state; (b) heated at 500 °C under flowing oxygen; (c) cooled to 50 °C under flowing oxygen.

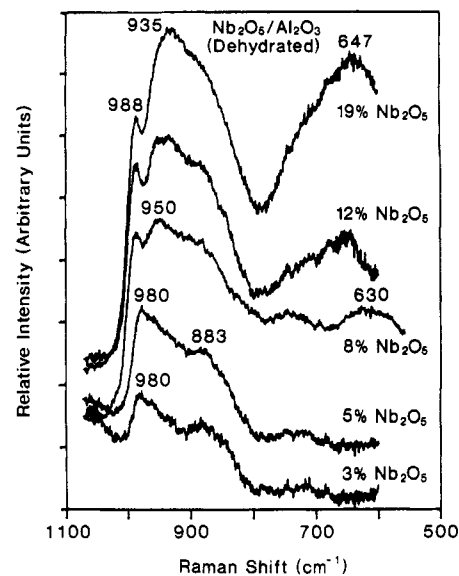


Figure 9. In situ Raman spectra of the $\text{Nb}_2\text{O}_5/\text{Al}_2\text{O}_3$ system as a function of Nb_2O_5 loading.

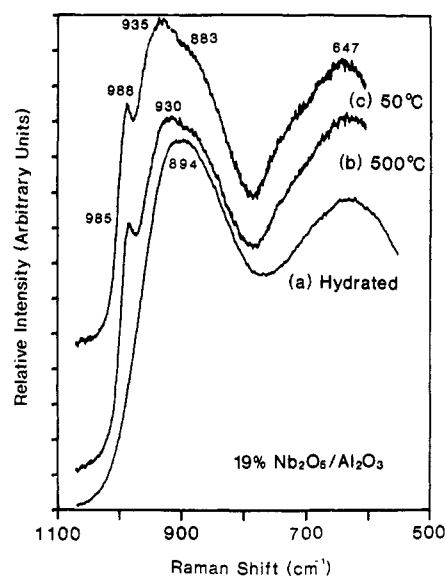


Figure 8. In situ Raman spectra of 19 wt % $\text{Nb}_2\text{O}_5/\text{Al}_2\text{O}_3$: (a) hydrated state; (b) heated at 500 °C under flowing oxygen; (c) cooled to 50 °C under flowing oxygen.

Raman bands at ~ 980 and ~ 883 cm^{-1} are present and their intensity increases with Nb_2O_5 loading. For the 8 wt % Nb_2O_5 loading, the Raman band at ~ 980 cm^{-1} shifts to ~ 988 cm^{-1} and new Raman bands appear at ~ 950 and ~ 630 cm^{-1} . Upon further increasing the Nb_2O_5 loadings (>8 wt %), the Raman bands originally occurring at ~ 950 and ~ 630 cm^{-1} shift to ~ 935 and ~ 647 cm^{-1} , respectively, and their intensity increases with Nb_2O_5 loading.

$\text{Nb}_2\text{O}_5/\text{MgO}$. The in situ Raman spectra of magnesia-supported niobium oxide, with 5 and 10 wt % Nb_2O_5 , are shown in Figures 10 and 11, respectively. The broad Raman band at ~ 870 cm^{-1} is associated with the supported niobium oxide phase under ambient conditions since MgO is not Raman active and increases with Nb_2O_5 loading. The Raman band at ~ 1085 cm^{-1} is due to a CaCO_3 impurity present in the MgO support. Under in situ conditions, the Raman band originally at ~ 870 cm^{-1} splits into bands at ~ 935 , ~ 892 , and ~ 833 cm^{-1} for the 5 wt % $\text{Nb}_2\text{O}_5/\text{MgO}$ sample and into bands at ~ 985 , ~ 898 , and ~ 834 cm^{-1} for the 10 wt % $\text{Nb}_2\text{O}_5/\text{MgO}$ sample. After the sample was exposed to ambient conditions for overnight, the broad Raman band at ~ 870 cm^{-1} reappeared due to the hydration of the surface niobium oxide phases by adsorbed moisture (see Figure 11).

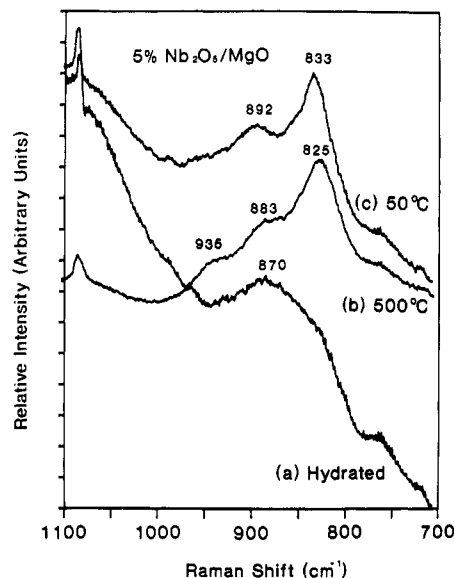


Figure 10. In situ Raman spectra of 5 wt % $\text{Nb}_2\text{O}_5/\text{MgO}$: (a) hydrated state; (b) heated at 500 °C under flowing oxygen; (c) cooled to 50 °C under flowing oxygen.

Discussion

Raman studies on supported niobium oxide catalysts reveal that niobium oxide is present as a two-dimensional surface overlayer on oxide supports below monolayer coverage.⁷ The two-dimensional surface niobium oxide overlayer possesses the major Raman bands in the 800–100- cm^{-1} region which are different than bulk crystalline Nb_2O_5 phases (major Raman band at ~ 690 cm^{-1}). Crystalline Nb_2O_5 phases are present above monolayer coverage and at elevated temperatures. The molecular structures of the surface niobium oxide phases under ambient conditions, where adsorbed water is present, can be determined by directly comparing their Raman spectra with those of niobium oxide aqueous solutions and are controlled by the surface pH.^{7,29} The surface pH is determined by the combined pH of the oxide support and the niobium oxide overlayer. The addition of surface niobium oxide (pH ~ 0.5) to oxide supports ($2 < \text{pH} < 12$) will decrease the surface pH, and the decrease will be proportional to the surface niobium oxide coverage. At low surface niobium oxide coverages of supported niobium oxide catalysts, the surface pH under ambient conditions is dominated by the properties of the oxide

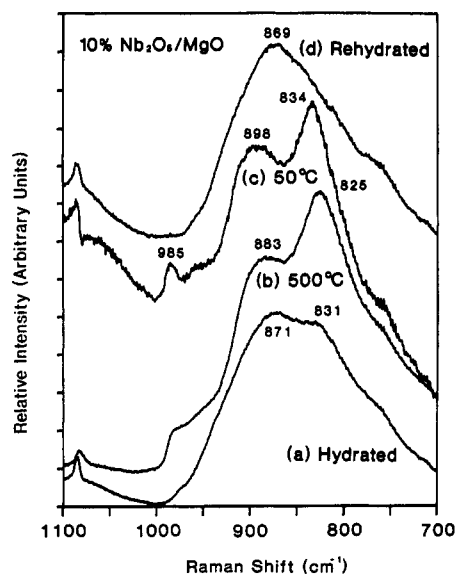


Figure 11. In situ Raman spectra of 10 wt % $\text{Nb}_2\text{O}_5/\text{MgO}$: (a) hydrated state; (b) heated at 500 °C under flowing oxygen; (c) cooled to 50 °C under flowing oxygen; (d) reabsorbed water molecules under ambient conditions.

support. The basic pH values of the MgO, pH = 12, and Al_2O_3 , pH = 9, supports suggest that hexaniobate species ($\text{H}_x\text{Nb}_6\text{O}_{19}^{-(6-x)}$, where $x = 1, 2, 3$) should be present with corresponding Raman bands at $\sim 880 \text{ cm}^{-1}$.²⁹ The somewhat acidic pH values of the TiO_2 , pH = 6.0–6.4, and ZrO_2 , pH = 4–7, supports suggest that $\text{Nb}_2\text{O}_5 \cdot n\text{H}_2\text{O}$ type structures, containing slightly distorted NbO_6 as well as NbO_7 and NbO_8 groups, should be present at $\sim 650 \text{ cm}^{-1}$ for $\text{Nb}_2\text{O}_5/\text{TiO}_2$ and $\text{Nb}_2\text{O}_5/\text{ZrO}_2$ at low surface coverages. Unfortunately, the strong vibrations of the TiO_2 and ZrO_2 supports in this region do not allow direct confirmation of such niobium oxide species. However, the rather weak Raman bands for $\text{Nb}_2\text{O}_5/\text{TiO}_2$ and $\text{Nb}_2\text{O}_5/\text{ZrO}_2$ at ~ 895 and $\sim 875 \text{ cm}^{-1}$ (see Figures 3a and 5a), respectively, are consistent with this conclusion. For the acidic SiO_2 support with a pH value of ~ 3.9 , $\text{Nb}_2\text{O}_5 \cdot n\text{H}_2\text{O}$ type structures with Raman band at $\sim 650 \text{ cm}^{-1}$ would be expected, but a weak and broad Raman band appearing at $\sim 960 \text{ cm}^{-1}$ instead of $\sim 650 \text{ cm}^{-1}$ is observed (see Figure 1a). This indicates that the surface niobium oxide phase on silica after treatment at 500 or 600 °C calcination contains a highly distorted NbO_6 octahedron which is similar to the "capping" structure of layered niobium oxide reference compound.³⁰ The transformation of the structure of the surface niobium oxide phase, from a slightly distorted NbO_6 octahedron to a highly distorted NbO_6 octahedron, on SiO_2 under high-temperature treatments is probably due to the weak interaction between the surface niobium oxide phase and the SiO_2 support, and the hydrophobicity of SiO_2 . At high surface coverages on basic (Al_2O_3) and acidic (TiO_2 and ZrO_2) oxide supports, hydrated niobium oxide type surface species ($\text{Nb}_2\text{O}_5 \cdot n\text{H}_2\text{O}$) are also present. The hydrated niobium oxide type surface species contain slightly distorted NbO_6 octahedra as well as slightly distorted NbO_7 and NbO_8 structures. In addition, bulk Nb_2O_5 Raman band at $\sim 680 \text{ cm}^{-1}$ was observed for 4 wt % $\text{Nb}_2\text{O}_5/\text{SiO}_2$, indicating that a monolayer coverage had been exceeded.

Under in situ conditions the adsorbed moisture desorbs upon heating and the surface metal oxide overlayers on the oxide supports become dehydrated.^{8–10,30} The molecular structures of the surface metal oxide phases are generally altered upon dehydration because the surface pH can only exert its influence via an aqueous environment. Consequently, Raman shifts upon dehydration constitute direct proof of a two-dimensional surface metal oxide phase and the removal of coordinated water.^{8–10,30}

The Raman band positions of the supported niobium oxide catalysts under in situ conditions (spectra were taken at 50 °C

TABLE I: Raman Bands of Supported Niobium Oxide Catalysts under in Situ Conditions (Dehydrated State)

	Raman bands, cm^{-1}
5% $\text{Nb}_2\text{O}_5/\text{MgO}$	930 (w), 892 (m), 833 (s)
10% $\text{Nb}_2\text{O}_5/\text{MgO}$	985 (m), 898 (s), 834 (s)
5% $\text{Nb}_2\text{O}_5/\text{Al}_2\text{O}_3$	980 (s), 883 (m)
19% $\text{Nb}_2\text{O}_5/\text{Al}_2\text{O}_3$	988 (m), 935 (s), 883 (w), 647 (s)
1% $\text{Nb}_2\text{O}_5/\text{TiO}_2$	983 (m)
7% $\text{Nb}_2\text{O}_5/\text{TiO}_2$	985 (s), 935 (m)
1% $\text{Nb}_2\text{O}_5/\text{ZrO}_2$	956 (s), 823 (s)
5% $\text{Nb}_2\text{O}_5/\text{ZrO}_2$	988 (s), 935 (m)
2% $\text{Nb}_2\text{O}_5/\text{SiO}_2$	980 (s)
4% $\text{Nb}_2\text{O}_5/\text{SiO}_2$	980 (s), 680 (m)

in a closed cell after being heated to 500 °C in flowing oxygen with the exception of the $\text{Nb}_2\text{O}_5/\text{SiO}_2$ spectra which were taken at 500 °C) are presented in Table I. The Raman positions of the surface niobium oxide phases at 50 °C usually occur at 2–3 cm^{-1} higher than at 500 °C due to the slight influence of temperature upon the Nb=O bond lengths. Upon dehydration, the surface niobium oxide Raman bands above 800 cm^{-1} experience a shift and the surface niobium oxide Raman bands between 600 and 700 cm^{-1} are not perturbed. Thus, the Raman bands appearing above 800 cm^{-1} are associated with surface niobium oxide phases and Raman bands appearing between 600 and 700 cm^{-1} are associated with either bulk niobium oxide phases or surface phases that still possess coordinated moisture as hydroxyl groups. Multiple dehydrated surface niobium oxide species with Raman bands in the 800–1000- cm^{-1} region are present in the supported niobium oxide catalysts.

On the SiO_2 support, only one dehydrated surface niobium oxide species with a sharp Raman band at $\sim 980 \text{ cm}^{-1}$ is observed, and no additional surface niobium oxide phases possessing Raman bands in the 880–950- cm^{-1} region are present. A Raman band at $\sim 980 \text{ cm}^{-1}$ is generally observed for highly distorted NbO_6 octahedra³⁰ and is also present at the interfaces of layered niobium oxide compounds.^{30,31} Recent structural studies of the supported niobium oxide catalysts also suggest that the dehydrated surface niobium oxide species, which exhibits a sharp Raman band at $\sim 980 \text{ cm}^{-1}$, can only possess one terminal Nb=O bond, because the Nb^{5+} atom cannot accommodate two terminal Nb=O bonds and should contain a highly distorted NbO_6 octahedral structure.³² Consequently, the dehydrated surface niobium oxide phase on SiO_2 is present as the highly distorted NbO_6 octahedron. An additional Raman band at $\sim 680 \text{ cm}^{-1}$ is observed for 4 wt % $\text{Nb}_2\text{O}_5/\text{SiO}_2$, but this is assigned to a bulk Nb_2O_5 phase because its band position is very close to T- Nb_2O_5 ($\sim 690 \text{ cm}^{-1}$) and it readily crystallizes upon heating to elevated temperatures.⁷

A Raman band at $\sim 985 \text{ cm}^{-1}$ is also observed for the dehydrated titania- and zirconia-supported niobium oxide catalysts and is also assigned to the highly distorted NbO_6 octahedra. The somewhat lower Raman band positions of the dehydrated 1% $\text{Nb}_2\text{O}_5/\text{ZrO}_2$ sample are attributed to the presence of surface Cl and F impurities which were detected with XPS only in this particular sample. Upon approaching monolayer coverage, an additional Raman band at $\sim 935 \text{ cm}^{-1}$ is observed for the dehydrated titania- and zirconia-supported niobium oxide catalysts and is also assigned to a highly distorted NbO_6 octahedron with a slightly longer Nb=O bond.

On the dehydrated Al_2O_3 support, Raman bands at ~ 980 and $\sim 883 \text{ cm}^{-1}$ are observed for the low Nb_2O_5 loadings (see Figure 5), indicating the presence of two kinds of distorted NbO_6 octahedral structure: one possesses a Nb=O bond length similar to layered niobium oxide compounds and the other possesses a Nb=O bond length similar to that found in hexaniobate, $\text{Nb}_6\text{O}_{19}^{8-}$, compounds.³⁰ At the surface coverage approaching half a monolayer ($\sim 8 \text{ wt } \%$), the Raman band at $\sim 980 \text{ cm}^{-1}$ shifts to $\sim 988 \text{ cm}^{-1}$ and indicates that the nature of the dehydrated

(30) Jehng, J. M.; Wachs, I. E. *Chem. Mater.* 1991, 3, 100.

(31) Jacobson, A. J.; Lewandowski, J. T.; Johnson, J. W. *J. Less-Common Metals* 1986, 116, 137.

(32) Hardcastle, F. D. Ph.D. Dissertation, Lehigh University; University Microfilms International: Ann Arbor, MI 1990.

surface niobium oxide species changes with surface coverage. New in situ Raman bands are observed at ~ 950 and ~ 630 cm^{-1} and are characteristic of the dehydrated surface niobium oxide species containing both highly and slightly distorted NbO_6 octahedral structures. These Raman bands are also observed for layered niobium oxide compounds which consist of both highly and slightly distorted NbO_6 octahedral structure connected by sharing corners.^{30,31} In addition, the shifts of Raman bands from ~ 950 to ~ 935 cm^{-1} and from ~ 630 to ~ 647 cm^{-1} upon approaching monolayer coverage also suggest that these two Raman bands arise from the same dehydrated surface niobium oxide species.

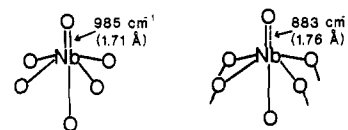
An in situ Raman band is present at ~ 890 cm^{-1} on the MgO support which reflects the presence of another distorted NbO_6 octahedron that possesses a $\text{Nb}=\text{O}$ bond length similar to that found in the MgNb_2O_6 compound.^{33,34} The absence of crystalline Nb_2O_5 formation for $\text{Nb}_2\text{O}_5/\text{MgO}$ at very high niobium oxide loadings suggests that this species originates from Nb^{5+} incorporated into the MgO support surface due to the strong acid-base interaction between these two oxides. Recent Raman studies on the MgO supported molybdenum oxide catalysts have found that the MgO support contains CaCO_3 on the surface, and the amount of CaCO_3 decreases with increasing molybdenum oxide loading because of the formation of CaMoO_4 .³⁵ Similar to the MoO_3/MgO system, the formation of the $\text{Ca}_2\text{Nb}_2\text{O}_7$ compound is due to the reaction of the acidic niobium oxide with CaCO_3 present on the MgO surface. The dehydrated $\text{Nb}_2\text{O}_5/\text{MgO}$ sample also possesses additional Raman bands at ~ 833 and ~ 770 cm^{-1} which coincide with the Raman positions of a distorted NbO_6 octahedral structure present in the $\text{Ca}_2\text{Nb}_2\text{O}_7$ compound.³⁶ No Raman feature at ~ 980 cm^{-1} for the 5 wt % $\text{Nb}_2\text{O}_5/\text{MgO}$ sample indicates that a highly distorted surface NbO_6 species, which was observed in the $\text{Nb}_2\text{O}_5/\text{SiO}_2$, $\text{Nb}_2\text{O}_5/\text{TiO}_2$, $\text{Nb}_2\text{O}_5/\text{ZrO}_2$, and $\text{Nb}_2\text{O}_5/\text{Al}_2\text{O}_3$ systems, is not present on the MgO support. However, the Raman features of the supported niobium oxide on MgO are affected by hydration/dehydration procedures due to the hydrophilicity of MgO (the formation of $\text{Mg}(\text{OH})_2$ upon exposure to moisture). XRD does not detect the crystalline MgNb_2O_6 and $\text{Ca}_2\text{Nb}_2\text{O}_7$ phases present in the $\text{Nb}_2\text{O}_5/\text{MgO}$ system suggest that the particle size of the crystalline phases are smaller than 40 Å.

On the dehydrated MgO support, multiple niobium oxide species possessing Raman bands in the 800–900- cm^{-1} region are present due to the strong acid-base interactions of Nb_2O_5 with the Mg^{2+} and the Ca^{2+} surface cations, and their intensity increases with the Nb_2O_5 loading. At high Nb_2O_5 loadings (>10 wt %), the Raman band at ~ 985 cm^{-1} is characteristic of a highly distorted NbO_6 octahedral structure which coexists with the MgNb_2O_6 and $\text{Ca}_2\text{Nb}_2\text{O}_7$ compounds (see Figure 11). This suggests that a surface niobium oxide overlayer with a "capping" structure of layered niobium oxide compound³⁰ is probably formed on the more acidic MgNb_2O_6 and $\text{Ca}_2\text{Nb}_2\text{O}_7$ surfaces.

The molecular structures of the dehydrated surface niobium oxide species with their corresponding bond lengths are presented in Table II. The predicted bond lengths of each structure are obtained from an empirical $\text{Nb}-\text{O}$ bond distance/stretching frequency correlative equation which is derived by Hardcastle.³² Below half monolayer coverage, the highly distorted NbO_6 octahedra, with a $\text{Nb}=\text{O}$ bond length of 1.71 Å, are present on all the dehydrated oxide supports. On the Al_2O_3 support, a second dehydrated surface niobium oxide species possessing a moderately distorted NbO_6 octahedral structure, with a $\text{Nb}=\text{O}$ bond length of 1.76 Å, is also present. As monolayer coverage is approached, additional dehydrated surface niobium oxide species with structures similar to layered niobium oxide compounds, which contain both highly distorted NbO_6 octahedra with a $\text{Nb}=\text{O}$ bond length

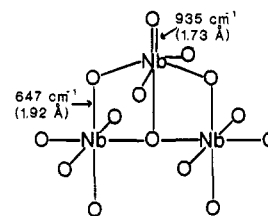
TABLE II: A Plausible Model for Molecular Structures of the Dehydrated Surface Niobium Oxide Species

• Below half a monolayer coverage:



Highly distorted NbO_6 octahedra with different $\text{Nb}=\text{O}$ bond distances

• Approaching monolayer coverage:



Highly and slightly distorted NbO_6 octahedra coexist in the structure

of 1.73 Å and slightly distorted NbO_6 octahedra with a $\text{Nb}-\text{O}$ bond length of 1.92 Å, are present on Al_2O_3 but not on SiO_2 and MgO . The dehydrated surface niobium oxide phases possessing Raman bands in the 600–700- cm^{-1} region may be present for $\text{Nb}_2\text{O}_5/\text{TiO}_2$ and $\text{Nb}_2\text{O}_5/\text{ZrO}_2$ but cannot be determined by Raman spectroscopy because of the strong vibrations of the oxide supports in this region. Layered niobium oxide compounds react with the weak base pyridine, which indicates that these compounds possess strong Brønsted acid sites due to the presence of H^+ protons in the adjacent terminal oxygen layers.³¹ Thus, surface acidic studies on TiO_2 and ZrO_2 supported niobium oxide catalysts with FTIR of pyridine adsorption can provide additional information for determining the molecular structures of the dehydrated surface niobium oxide species on these two systems.

In situ XANES/EXAFS studies on the silica-supported niobium oxide catalysts containing different Nb_2O_5 loadings have been reported by Yoshida et al. using YbNbO_4 and KNbO_3 as the reference compounds.²⁶ They suggest that the dehydrated surface niobium oxide phase possesses a highly distorted NbO_4 tetrahedron at low Nb_2O_5 loadings (<1 wt %) and a square pyramidal structure at high Nb_2O_5 loadings (>7 wt %). The proposed dehydrated surface tetrahedral NbO_4 structure consists of one terminal $\text{Nb}=\text{O}$ bond, with a bond length of 1.77 Å, and three $\text{Nb}-\text{O}$ bonds, with a bond length of 1.96 Å, coordinated to the SiO_2 surface. At high Nb_2O_5 loadings (>7 wt %), the proposed dehydrated surface niobium oxide structure consists of one terminal $\text{Nb}=\text{O}$ bond, with a bond length of 1.79 Å, and four $\text{Nb}-\text{O}$ bonds, with a bond length of 1.96 Å, coordinated to the SiO_2 surface. The XANES/EXAFS studies on the YbNbO_4 reference compound are in agreement with corresponding Raman studies that YbNbO_4 consists of a tetrahedral NbO_4 structure.³⁰ KNbO_3 is known as a perovskite structure containing a slightly distorted NbO_6 octahedral structure with $\text{Nb}-\text{O}$ bond lengths between 1.87 and 2.17 Å.^{30,32} The Raman bands of KNbO_3 occur at ~ 840 , ~ 601 , ~ 540 , and ~ 285 cm^{-1} .³⁰ Thus, XANES/EXAFS studies on KNbO_3 are not representative of a dehydrated surface niobium oxide species which possess a highly distorted NbO_6 octahedral structure. Clearly, additional niobium oxide reference compound XANES/EXAFS studies are required.

The feasibility of Yoshida's model for the dehydrated surface niobium oxide structures is investigated by applying Brown and Wu's valence sum rule.³⁷ The sum of the valencies, or bond orders, of the individual metal-oxygen bonds should equal the formal oxidation state of the metal cation. The calculated valence state of the Nb^{5+} atom for the NbO_4 tetrahedron proposed by Yoshida is 4.07 v.u. which is beyond the limit of the 3% relative error allowed for the Nb^{5+} valence state (5.0 ± 0.16 v.u.), and

(33) Husson, E.; Repelin, Y.; Dao, N. Q.; Brusset, H. *Mater. Res. Bull.* **1977**, *12*, 1199.

(34) Husson, E.; Repelin, Y.; Dao, N. Q.; Brusset, H.; Fardouet, E. *Spectrochim. Acta* **1977**, *33A*, 995.

(35) Williams, C. C.; Ekerdt, J. G.; Jehng, J. M.; Hardcastle, F. D.; Wachs, I. E., submitted to *J. Phys. Chem.*

(36) Jehng, J. M.; Wachs, I. E., unpublished work.

(37) Brown, I. D.; Wu, K. K. *Acta Crystallogr.* **1976**, *B32*, 1957.

that for the NbO_5 square pyramidal also proposed by Yoshida is 4.86 v.u. which is under the limit of the 3% relative error. The Nb–O bond distance/stretching frequency correlation derived by Hardcastle³² can also be used to predict the Raman band position of the dehydrated surface niobium oxide on the SiO_2 support for the structure proposed by Yoshida. The predicted Nb–O stretching frequency, corresponding to the bond distances of 1.77, 1.79, and 1.96 Å proposed by Yoshida, would appear at ~ 870 , ~ 840 , and $\sim 605 \text{ cm}^{-1}$ ($\pm 30 \text{ cm}^{-1}$ error). This predicted Raman band is not consistent with the present study in which the dehydrated surface niobium oxide on the SiO_2 support is experimentally shown to possess a Raman band at $\sim 980 \text{ cm}^{-1}$. At high Nb_2O_5 loading, the predicted Raman bands at ~ 840 and $\sim 605 \text{ cm}^{-1}$ for the structure proposed by Yoshida are consistent with the presence of bulk Nb_2O_5 (see Figure 2). In addition, the ratio of the Nb^{5+} ionic radius to the O^{2-} ionic radius is too large to fit into a NbO_4 tetrahedral structure and a NbO_6 octahedral structure is more plausible.³⁸ Thus, all the theories and experiments indicate that the dehydrated surface niobium oxide phases are not very likely to possess a NbO_4 tetrahedral structure.

The various dehydrated surface niobium oxide structures present in supported niobium oxide catalysts appear to be related to the oxide support surface hydroxyl chemistry.³⁹ The surface niobium oxide phases are formed by reaction of the niobium oxide precursor with the surface hydroxyl groups of the oxide supports which are directly observable with infrared spectroscopy.^{40,41} The SiO_2 surface possesses only one kind of surface hydroxyl group and only one dehydrated surface niobium oxide species (Raman band at $\sim 980 \text{ cm}^{-1}$) is present. The TiO_2 and ZrO_2 surfaces possess two kinds of surface hydroxyl groups and two dehydrated surface niobium oxide species (Raman band at ~ 985 and $\sim 935 \text{ cm}^{-1}$) are present. The Al_2O_3 surface possesses at least four different surface hydroxyl groups and three dehydrated surface niobium oxide species (Raman bands at ~ 985 , ~ 935 , ~ 880 , and $\sim 647 \text{ cm}^{-1}$) present. The MgO surface possesses one kind of surface hydroxyl group, but three different niobium oxide species are observed (Raman bands at ~ 985 , ~ 890 , and $\sim 830 \text{ cm}^{-1}$) under in situ conditions. The multiple niobium oxide species present in the dehydrated $\text{Nb}_2\text{O}_5/\text{MgO}$ system are due to the strong acid–base interaction between Nb_2O_5 and MgO which results in the incorporation of niobium oxide into the MgO support surface

and the reaction of Nb_2O_5 with CaCO_3 which is present on the MgO surface. The low surface hydroxyl concentration of the SiO_2 support,³⁹ relative to the other oxide supports, is responsible for the low surface concentration of surface niobium oxide species and the formation of bulk Nb_2O_5 at very low niobium oxide loadings.

Conclusions

The molecular structures of the dehydrated surface niobium oxide phases were determined with in situ Raman spectroscopy by comparing the Raman spectra of the supported niobium oxides with those of solid niobium oxide reference compounds. Under in situ conditions, the adsorbed moisture desorbs upon heating and the surface niobium oxide overlayers on oxide supports become dehydrated. The dehydration process further distorts the highly distorted NbO_6 octahedra and shifts the surface niobium oxide Raman bands in the $890\text{--}910\text{-cm}^{-1}$ region to $930\text{--}990\text{-cm}^{-1}$ region because of the removal of the coordinated water.

A dehydrated surface niobium oxide Raman band is observed at $\sim 985 \text{ cm}^{-1}$ on all the oxide supports and reveals that the same surface niobium oxide species possessing a highly distorted NbO_6 octahedral structure is present for all the supported niobium oxide catalysts. Below half a monolayer coverage on the Al_2O_3 support, a second dehydrated surface niobium oxide species possessing a highly distorted NbO_6 octahedral structure with a somewhat longer Nb=O bonds ($\sim 883 \text{ cm}^{-1}$) is also present. Upon approaching monolayer coverage on the Al_2O_3 support, additional Raman bands at ~ 935 and $\sim 647 \text{ cm}^{-1}$ are observed which are characteristic of highly and slightly distorted NbO_6 octahedra similar to those present in layered niobium oxide compounds.

The highly distorted NbO_6 octahedra exhibiting a Raman band at $\sim 935 \text{ cm}^{-1}$ are also observed on the TiO_2 and ZrO_2 supports; however, surface niobium oxide phases possessing Raman bands in the $600\text{--}700\text{-cm}^{-1}$ region cannot be determined for $\text{Nb}_2\text{O}_5/\text{TiO}_2$ and $\text{Nb}_2\text{O}_5/\text{ZrO}_2$ because of the strong vibrations of the oxide supports in this region. On the SiO_2 support, only one dehydrated surface niobium oxide species possessing the highly distorted NbO_6 octahedral structure is found. The multiple niobium oxide species present in the $\text{Nb}_2\text{O}_5/\text{MgO}$ system are due to the strong acid–base interaction of Nb_2O_5 with the Mg^{2+} and the Ca^{2+} cations present on the surface to form MgNb_2O_6 and $\text{Ca}_2\text{Nb}_2\text{O}_7$. The various dehydrated surface niobium oxide species present in the supported niobium oxide catalysts appear to be related to the oxide support surface hydroxyl chemistry.

Acknowledgment. Financial support for this work by Niobium Products Company Inc. is gratefully acknowledged.

(38) Pauling, L. *General Chemistry*; Dover: New York, 1988.

(39) Yin, Y. S.; Ougour, A.; Auroux, A.; Vederine, J. C. *Stud. Surf. Sci. Catal.* **1989**, *48*, 525.

(40) Turek, A.; Wachs, I. E.; DeCanio, E., to be published.

(41) Datka, J.; Turek, A.; Jehng, J. M.; Wachs, I. E. *J. Catal.*, in press.